CHAPTER 3
STRESS STATE IN THE SLOPE AFTER MINING

3.1 SUMMARY

This chapter deals with the stress state of a slope profile situated above undulating strata such that the strata dip towards the toe of the slope. A relatively weak layer is present in the succession, and could be either a shale layer in sandstone or coal pillars left underground. It is shown that direct application of the Mohr-Coulomb shear failure criterion does not give satisfactory results in specific conditions when the artificial cut is made above the trough of the undulated strata. Attention is drawn to the stress difference between the virgin conditions and after slope excavation, as modelled by FLAC. The general case is discussed in Appendix 1.2. Profile lines along the bottom contact between the embedded shale layer and the sandstone aid all discussions where failures were observed in the colliery slopes. The existence of a negative stress difference along the bottom contact of the shale is demonstrated, which indicates stress relaxation in the shale layer compared to the virgin conditions. In the case of underground pillars we have a decrease of the vertical pillar stress difference, indicating decreased loading on the pillars during surface mining, compared with the pillar stresses after underground mining was complete. It is standard surface mining practice to buffer-blast the pillars from surface, to remove the possibility of later pillar collapse once the slope has been cut. Buffer blasting

is tantamount to pillar collapse, and since it does not cause slope instability, it is concluded that collapsed pillars at the slope toe will almost certainly not be responsible for slope instability.

3.2 INTRODUCTION

Chapter 2 dealt with pre-mining stress variations along three profile lines in undulating strata (see Figures 2.3 and 2.9). As was pointed out in Chapter 1, in all cases, the failure surface responsible for the slope instabilities was observed on the bottom contact between the shale layer and the relatively stronger middle coal seam underlying it. It is widely accepted that the stress component normal to the failure surface is the main parameter governing the failure. For this reason, this chapter concentrates on this stress component.

This chapter starts with an analysis of the effect of a high k-ratio on the failure potential in a cut slope on the shale-middle coal seam contact, and then continues with a discussion of slope profile scenarios with limb inclinations of 5^0 and 15^0.

3.3 EFFECT OF HIGH K-RATIO ON FAILURE POTENTIAL

In Section 2.4, we discussed the reasons for the choice of the k-factor, and settled on k=2 for all model analyses. The virgin stress state in any failure scenario is a very important parameter, and the question now is: will a virgin stress state in which

the horizontal stress is twice the vertical stress favour failure along the contact surface between the shale layer and the middle coal seam once a mined slope is present?

In order to answer this question, a mined slope with single terrace 30 m high, and slope angle of 70^0 was modelled using DIGS (Discontinuity Interaction and Growth Simulation, CSIR, 1996). This code, based on a boundary element method, simulates fracture propagation in a homogeneous body, assuming one of the fracture propagation modes (e.g. tensile, or shear). The code was set to model shear failure in a homogeneous mudstone with properties listed for the shale in Table 2.1, since the model cannot take account of the anisotropic laminated nature of shale.

The model geometry was kept as simple as possible, with the pure objective of answering the above question, rather than developing a complex geometry that was similar to the pre-failure geometries seen in Chapter 1. In the three scenarios modelled the virgin k-ratio was set at 0.5, 1.0, and 2.0 (see Figure 3.1).

Firstly, the model predicts the formation of a shear fracture that propagates from just below or just above the toe of the slope, backwards into the slope, curving upwards towards the surface. This is similar to a circular failure mechanism. As the *k*-ratio increases above 1.0, the predominantly circular failure mechanism becomes flatter and lies closer to the failure surface on the top contact of the middle coal seam observed at the coal mine.

a)

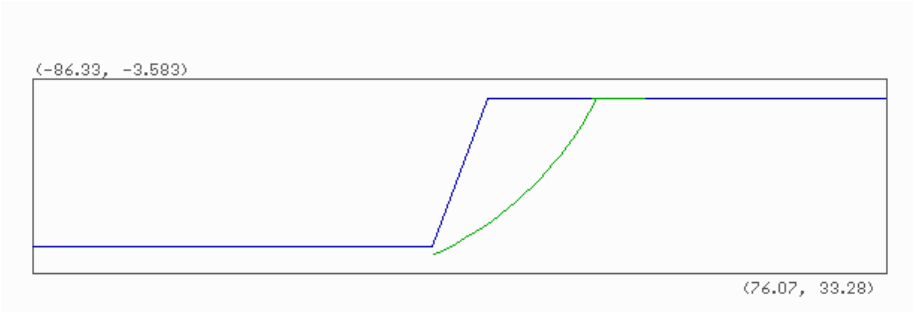

b)

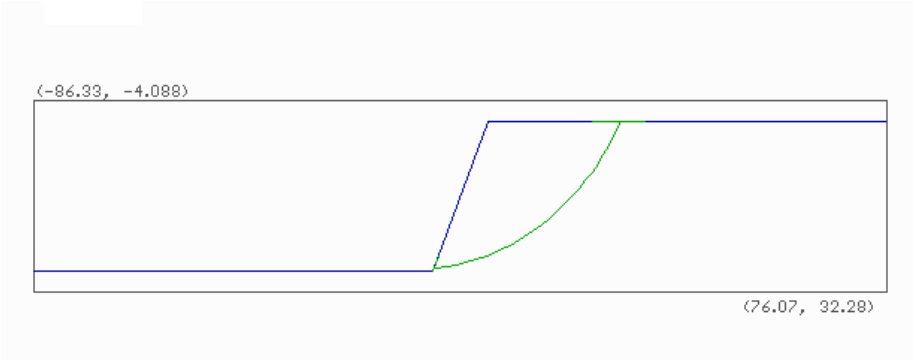

c)

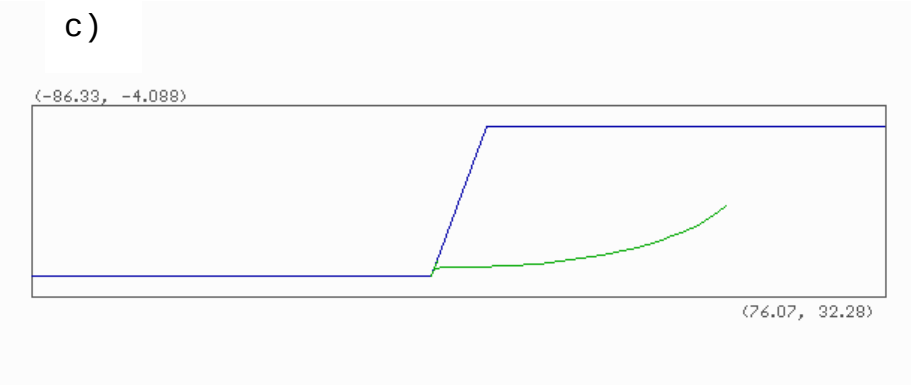

Figure 3.1

Shear fracture propagation in homogeneous slope profile with virgin stress ratio of: a) k=0.5; b) k=1.0 and c) k=2.0

This model does not confirm absolutely that failure along the shale-middle coal seam contact will actually take place, because of its geometric simplicity, and inability to model undulating anisotropic strata. However, it does confirm that shear failure is more likely on the shale-coal contact when the virgin k-ratio is 2, than when the k-ratio is 0.5.

3.4 SIMPLIFIED FLAC MODEL FOR MINED SLOPE

Because of the complex geotechnical conditions, the FLAC^{2D} code (Itasca, 1999) was used to model stress conditions in the slope after a mining cut had been made. Rather than modelling the influence of every variable in the slope geometry, the author has relied on earlier studies in the literature for simple guidelines. Hoyaux and Ladanyi (1972) and Stacey (1970 and 1973) presented some valuable results regarding the stress distribution in a slope and the influence of the slope angle. Kitahara et al (1986) investigated in more detail the original stress state, which could have high horizontal values. Jiang and Xie (1988) investigated the stresses in a slope profile due to the dip of the strata. Griffiths and Lane (1999) presented examples of finite element slope stability analysis and compared it to the other solution methods. Despite their achievements regarding the stresses in a slope profile, the Griffiths and Lane (1999) models have horizontal strata with a constant thickness, which is uncommon in nature.

Owing to the inhomogeneous native rock structure typical of natural situations, there are differing

responses to the stress changes in different layers as a result of mining activity. These stress changes depend on the ratio of horizontal to vertical stresses, which also vary with depth. The important role of rock failure in slope stability analysis is also dependent on the accuracy of the model used. None of these effects can be adequately accounted for in the equilibrium methods discussed in Chapter 1, and none of the analyses described above are directly applicable to the problem at hand because they all assumed geotechnical simplicity to facilitate the analyses.

The mining cut to the middle coal seam is 45m wide (standard mining practice) and it is assumed that this is wide enough to nullify any effects of the slope on the other side of the cut. The model (as with the DIGS model above) therefore consists of a mine cut beginning at the left boundary, extending to a simplified mine cut slope in the middle of the model, with the original ground surface extending from the slope crest to the right-hand model boundary.

The mine slope is simplified to a single terrace slope, unlike the complexity of the mine slope profiles shown in Chapter 1. The reason for this is to develop a simple, yet viable finite difference model that can be used to investigate the influence of the geotechnical conditions in the slope, rather than the influence of mining details. The simplicity of the slope does not mask any critical details in the post-mining stress in the slope. The depth of the cut was assumed to be an average 30 m, similar to the dimensions of the slopes that failed. The simplified FLAC model has the same height, length and number of zones as the model

presented in Chapter 2. Once the effect of a simple cut and the geotechnical conditions on the post-mining stress state became known, more complex models which take mining details into account were developed. These models appear and are analysed in Chapter 6.

The undulating strata model under the slope occupies approximately 100m of the total 250m-grid length, which was designed to avoid any influence of the model boundaries on the stress state around the slope profile. There is one disadvantage to this model. During the course of application the FISH function does not accept any further “generate” commands, disregarding further changes in zone size or their coordinates for the purposes of mining slope simulation. Therefore, any slope face creation has to be done with line generation. After the “adjust” command, some of the zones might not have acceptable FLAC geometries, which causes grid failure and, as a consequence, failure of the model.

This event can be avoided by increasing the number of zones in the model, therefore improving approximation. More zones will reflect in longer runtime, however. The other option is to change coordinates on the crest of the slope and from there on the generated line, which will result in a slope angle of 69.5^0 or 71^0, instead of the intended 70^0.

Profile Line 1 (see Figure 2.9) is placed on the contact between the shale and the middle coal seam, and covers the 48m distance between the trough and the crest of the formation, where the failure surfaces were observed (Figures 1.1 and 1.8). The slope toe is

situated directly above the trough so that the strata in the slope dip toward the pit, as seen at the coal mine. Profile Line 2 is vertical and spans the distance between the shale-coal contact at the crest, and surface (Figure 2.9).

The properties for sandstone and shale listed in Tables 2.1 and 2.2 in Chapter 2 were used in the model for the appropriate strata in the geological succession. The properties of the middle coal seam are those listed in Table 3.1.

Table 3.1 Coal properties applied in the FLAC model

Geotechnical parameters	Properties
Bulk modulus – Pa	2.0E9
Shear modulus – Pa	8.5E8
Tensile strength – Pa	2.0E6
Cohesion – Pa	4.0E5
Friction angle – deg	27
Density – kg/m^3	1500

3.5 STRESS STATE IN THE SLOPE PROFILE AFTER MINING

The previous chapter developed a model of the expected virgin stress state in unmined ground, and the effects of an undulating formation on the stress state. This section will explore the stress state and possible failure modes in the mined slope using the Mohr-Coulomb failure criterion. Figures 3.2 and 3.3 demonstrate failure modes in the profile with a 70^0 slope and a 2m-thick embedded shale layer in flat strata and strata with a 5^0 limb inclination.

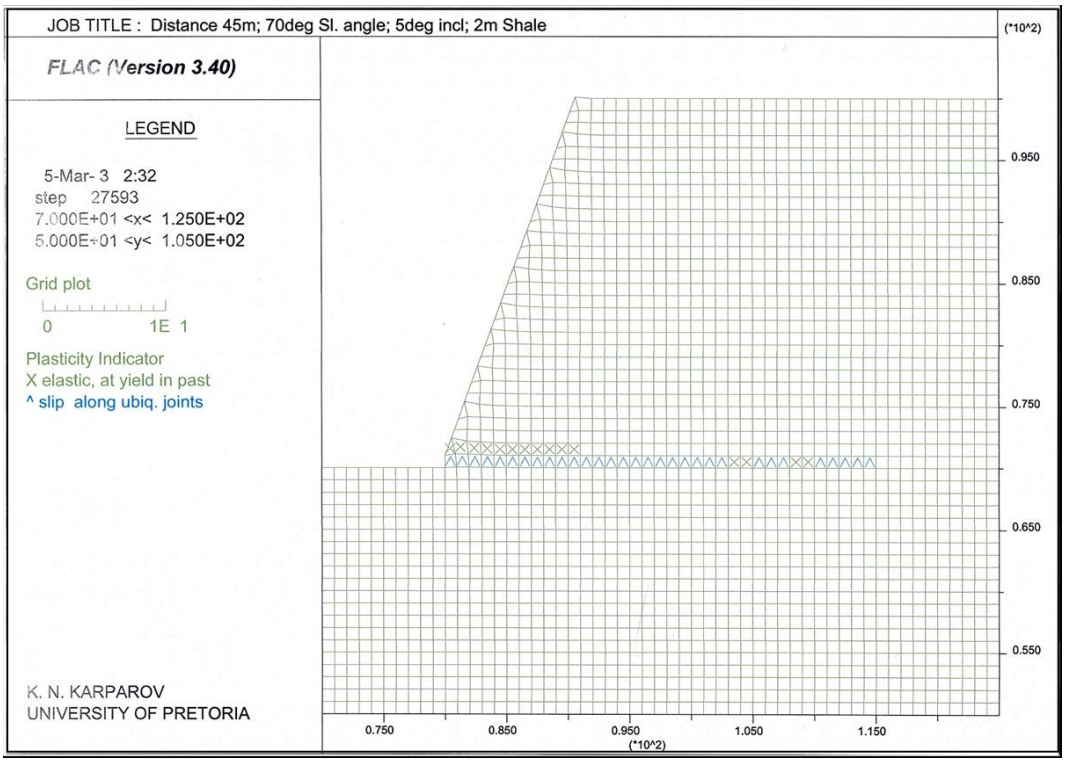

Figure 3.2

Failure in profile with flat strata

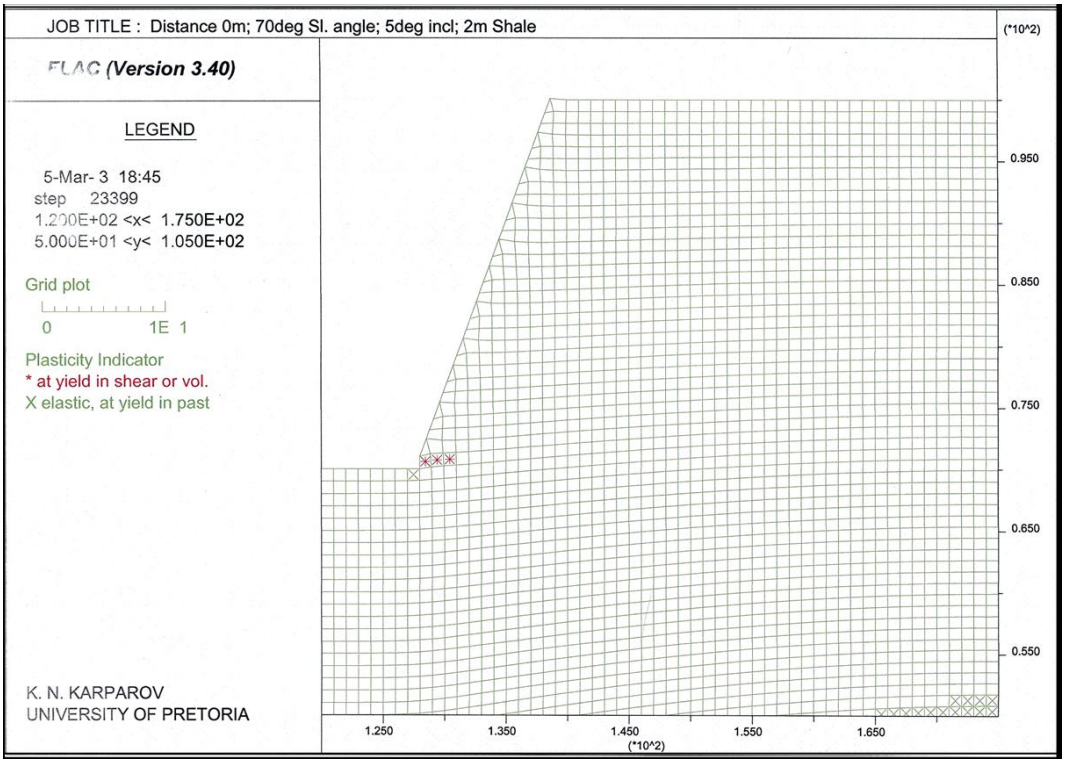

Figure 3.3

Failure in a slope with strata dipping at 5^0

In the flat layer scenario (Figure 3.2) we have an indication for slip along the weak bedding direction of approximately 30-35m, starting from the toe of the slope. The slope model shows some plastic deformations in the upper half of the embedded layer. Field observations show only layer swelling in such cases (Picture 1.1). In the case of the slope profile above the undulated strata (Figure 3.3), we have only plastic deformations in the first few metres from the toe of the slope.

Other slope profiles exhibit similar behaviour and their characteristics are given in Appendix 2 (Figures A2.7 to A2.10). Profiles with a vertical slope, which also exhibit the same behaviour, appear in the appendix (Figures A2.11-A2.16).

The major purpose of the failure models shown above and in Appendix 2 is to demonstrate that even when using a geotechnical model that contains the complexity of conditions seen at the mine, failure analyses produce inadequate results at best, and at worst, may be misleading (see Figures 3.2 and 3.3). Since the Mohr-Coulomb failure criterion was used in both models (the former demonstrating also slip along ubiquitous joints), they demonstrate that for failure to occur along the shale-coal contact, other mechanisms must also be involved. This is investigated in Chapter 4.

In Chapter 2 it was shown that induced stress differences in virgin conditions are caused by the undulated strata formation in the model. The influence of the presence of a mining cut is investigated in the following discussion. Figure 3.4 presents the vertical

stress difference (discussed in Appendix A1.2) along the profile line for a limb inclination of 15^0. It can be seen that there is a net tensile stress difference for some 30m into the slope from the toe for the 70^0 slope. The net induced tensile stress difference extends for a distance of only 10-12 m into the slope in the case of the vertical mine slope.

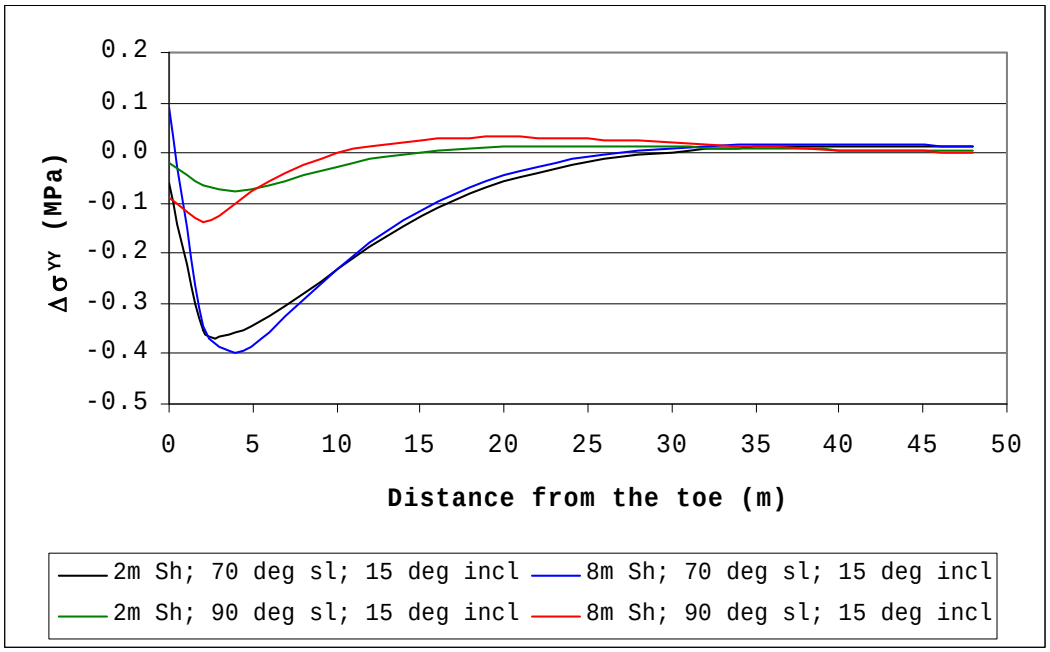

Figure 3.4

Vertical stress difference along profile line at shale–middle coal seam contact

The thickness of the shale layer has a less significant effect than the mine slope angle as demonstrated in Figure 3.4. Some compressive $\Delta\sigma_{YY}$ values develop in the first 1-2m from the toe of the slope, and are the result of the material failure there. The distances for which tensile $\Delta\sigma_{YY}$ values persist along the base of the shale layer for different cases are summarised in Table 3.2.

The results for the model with 5^0 limb inclination can be seen In Figure A3.2, Appendix 3, and are summarised in Table 3.2 below. The stress differences are mainly tensile for the profiles with flatter slope angles, and varying for different layer inclinations, and thicknesses. The resultant vertical stress component plots along the profile line can be seen in Figure A3.1, Appendix 3. It is concluded that the mining geometry is the dominant factor influencing the change in vertical stress along the profile line, and that the geotechnical factors such as layer thickness and limb inclination have relatively lesser influences.

Table 3.2 Distance that induced tensile stress $\Delta\sigma_{YY}$ persists into the slope along base of weak layer

Slope angle	5^0 Layer inclination	15^0 Layer inclination
2m thick shale layer		
70^0 slope angle	36m	26m
90^0 slope angle	20m	12m
8m thick shale layer		
70^0 slope angle	30m	24m
90^0 slope angle	8m	8m

The induced horizontal stress components along the shale-coal contact appear in Figure 3.5. They are the difference between the virgin values (Figure 3.10) and the resultant horizontal stress component (Figure A3.3, Appendix 3). In Figure 3.5 $\Delta\sigma_{XX}$ is shown only for the case of slope profiles with 15^0 limb inclination. In the figure all $\Delta\sigma_{XX}$ values have a negative sign for the slope profiles, indicating offloading along the whole profile line. The flatter formation exhibits similar results, which can be seen on Figure A3.4, Appendix 3.

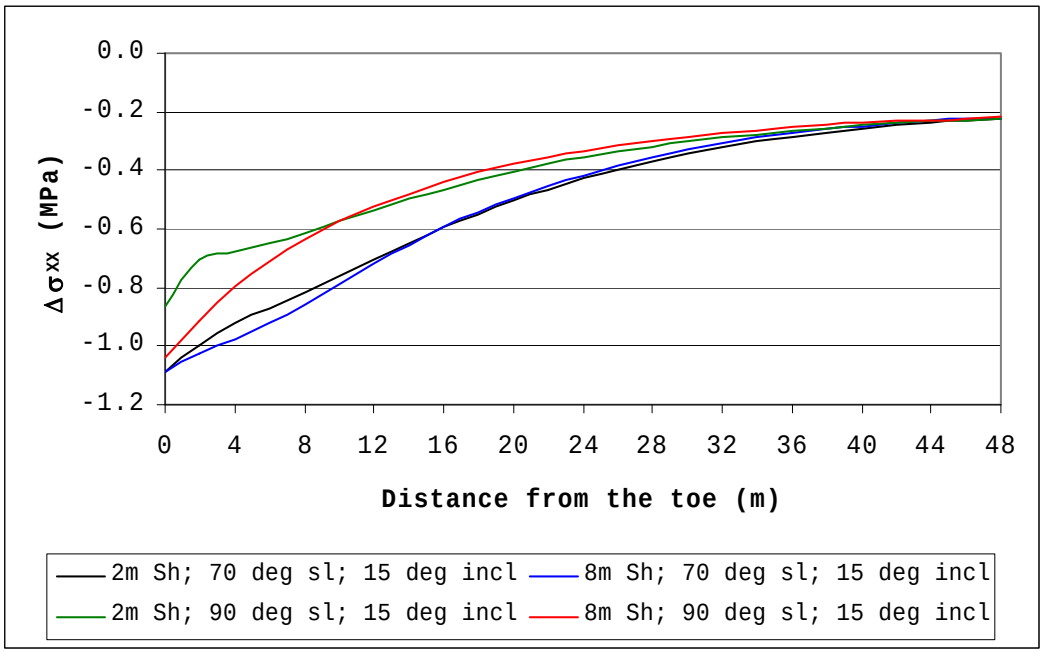

Figure 3.5
Horizontal stress difference along profile line at shale–middle coal seam contact

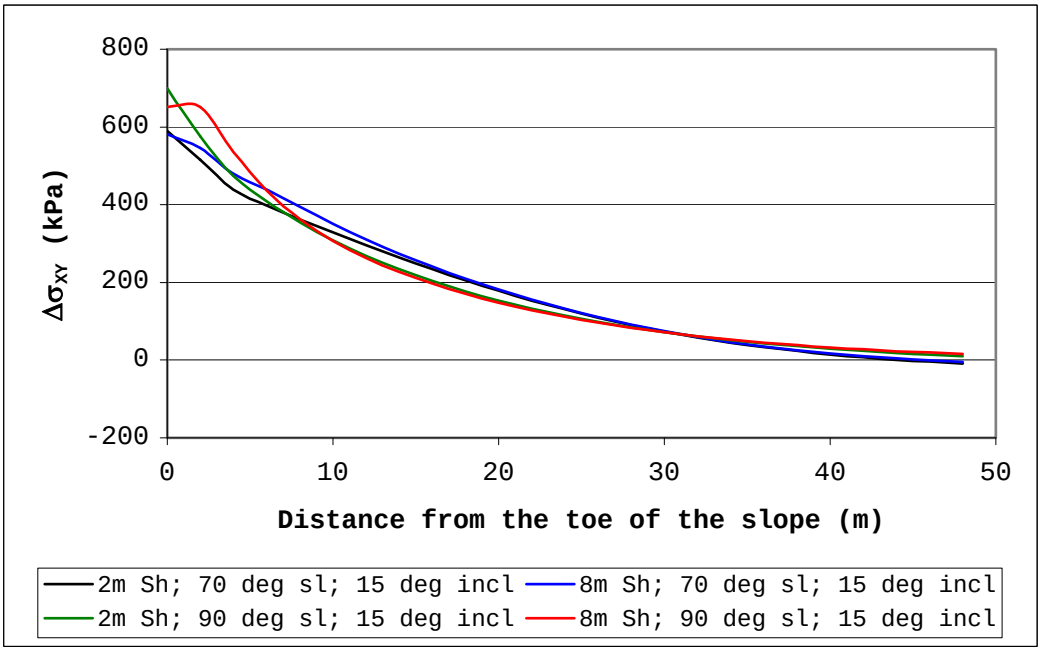

Figure 3.6
Shear stress difference along profile line on shale–middle coal seam contact

Figure 3.6 shows a plot of the shear stress difference induced by the presence of the mined slope. Firstly, it shows that there is a reversal in the sense of shear along the profile line until at least 30 m into the slope (compare Figures 2.14 and 3.6, noting that the toe of the slope coincides with the trough of the undulating formation), and that the magnitude of the induced shear stresses are much larger than those induced by the formation in virgin conditions. The induced shear stress results for the mined profiles with flatter formations in the model can be seen in Figure A3.6, Appendix 3.

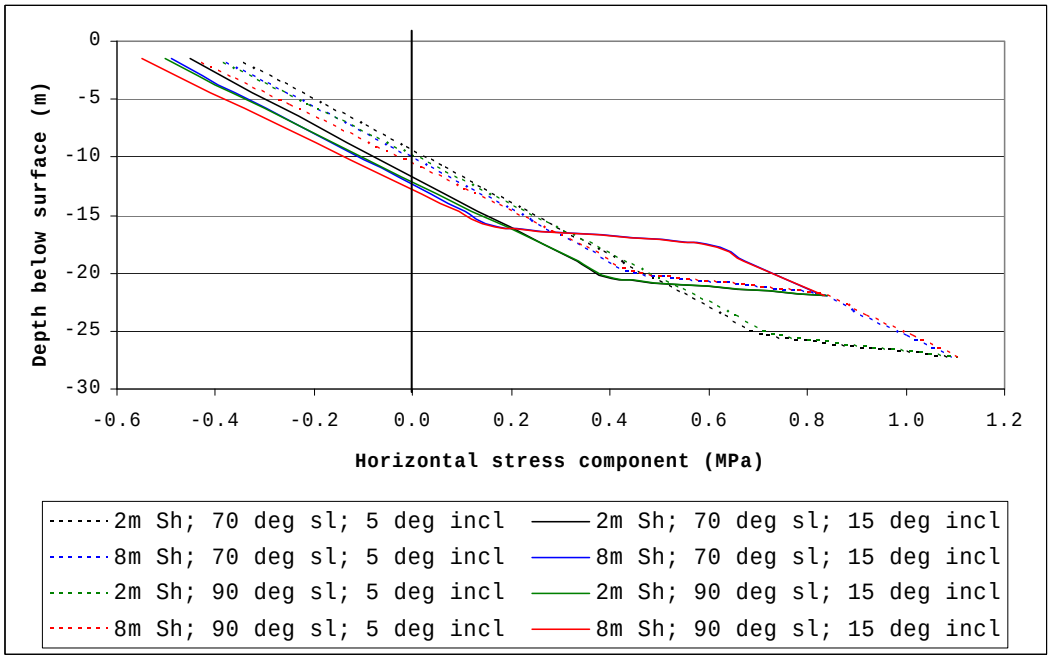

Figure 3.7
Horizontal stress component along a vertical profile line above the formation crest

Figure 3.7 presents a plot of the horizontal stress component along the vertical profile line above the crest of the formation when mining activities have taken place (refer to Figure 2.9 for position of

vertical profile line). There is a significant increase in the tensile stress component together with an increase in the tensile zone depth for all scenarios considered. Both the virgin and post-excavation stress states together with the tensile zone depth at the crest of the undulated strata formations are listed in Table 3.3 below. The significance of these results is that conditions conducive to surface tensile cracking are generated by a combination of mining and the subsurface geological structure.

Table 3.3 Maximum tensile stress and tensile zone depth along vertical line above formation crest

Slope angle (...^{0})	**Virgin stress (before mining)**		**Stress after mining**	
	Maximum Tensile stress (MPa)	**Tensile zone depth (m)**	**Maximum Tensile stress (MPa)**	**Tensile zone depth (m)**
5^0 limb inclination, 2m-thick shale layer				
70	-0.019	0.76	-0.399	8.73
90			-0.437	9.11
15^0 limb inclination, 2m-thick shale layer				
70	-0.140	3.42	-0.491	11.01
90			-0.533	11.39
5^0 limb inclination, 8m-thick shale layer				
70	-0.021	0.76	-0.433	9.49
90			-0.481	9.87
15^0 limb inclination, 8m-thick shale layer				
70	-0.143	3.42	-0.529	11.77
90			-0.579	12.15

Mining in particular brings about a significant increase in the magnitude of the maximum tensile stress as well as the depth to which it penetrates. The depth of the tensile zone and the magnitude of the maximum tensile stress are also influenced by the shale thickness, and in the case of the mined situation, slightly by the slope angle, but these factors are insignificant.

A little more detail on the horizontal stress state at surface is investigated next, because it will provide information on the potential for the formation of vertical tensile cracks behind the crest of the mined slope. These results are model predictions, and must not be assumed as guaranteed tensile horizontal stress at surface; the actual total stress at the surface will undoubtedly be neutral or slightly compressive, since surface soils would not be able to sustain any other stress state. Soils cope with induced tensile stresses by allowing the formation of tensile cracks commonly seen behind mining slope crests.

The results shown in Figures 2.15, 3.7, and 3.8 are specific to the modelled formation, since the depth of the formation below surface will have a strong influence on the surface tensile stress (i.e. if the formation were buried at a much greater depth than the modelled 30 metres, it should induce no horizontal tensile stress in the soils on surface or just below surface). Finally, we can assume that the thickness of the shale layer does not influence the horizontal stress component on the surface and that only the limb inclination does.

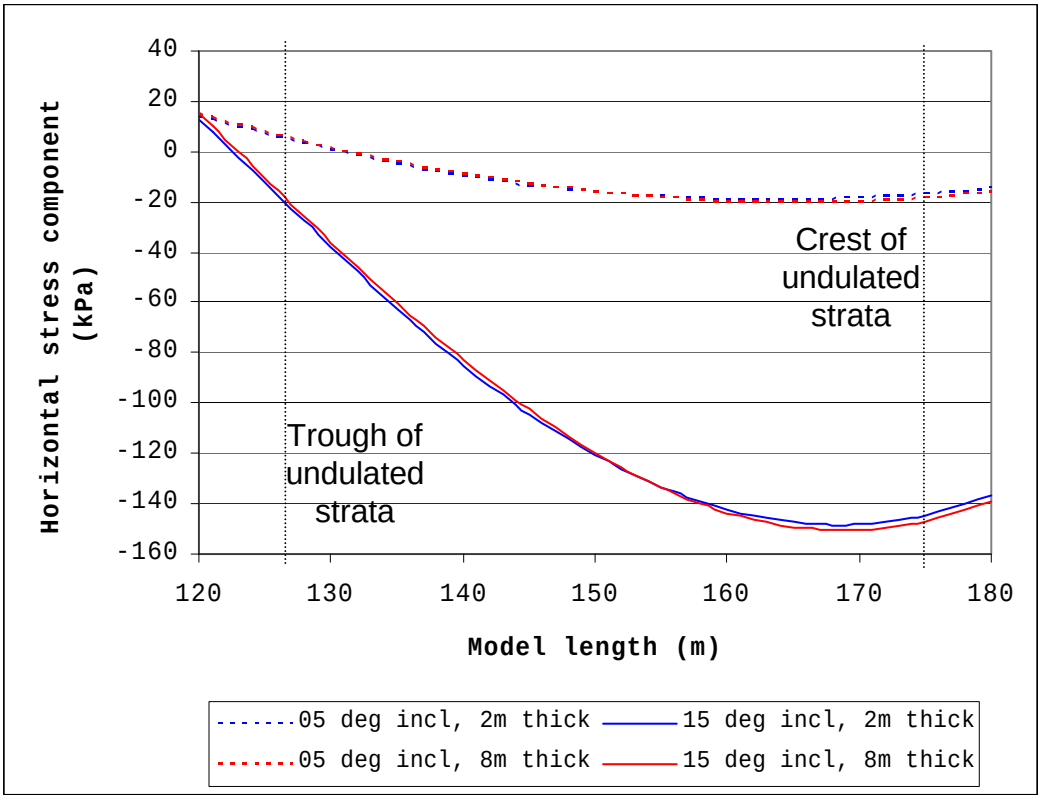

Figure 3.8
Horizontal stress component at surface

Thus far, all stresses have been expressed in terms of vertical and horizontal coordinates. Figure 3.9 shows the value of the stress difference ($\Delta\sigma_N$) normal to bedding along the shale-middle coal seam contact (see Figure 2.9) as calculated using Equation A1.9 (Appendix 1). In the figure, the $\Delta\sigma_N$ value has a negative sign, indicating a stress relaxation along the profile line for all cases.

The undulated strata formation with steeper limb inclination creates three to four times higher induced tensile ($\Delta\sigma_N$) values than the formation with flatter layer inclination. If we compare the graphs of the cases with different thickness of the layers then we

see that the thicker shale layer expresses slightly higher $\Delta\sigma_N$ in the first few metres than the profiles with a thinner shale layer.

The other most obvious difference between the graphs in Figure 3.9 is the comparison between $\Delta\sigma_N$ values of the profiles along the limb with different dip angles. The undulated strata formation with a flatter inclination angle exhibits smaller differences between the $\Delta\sigma_N$ values of the profiles with identical slope angle and layer thickness than the steeper formation does.

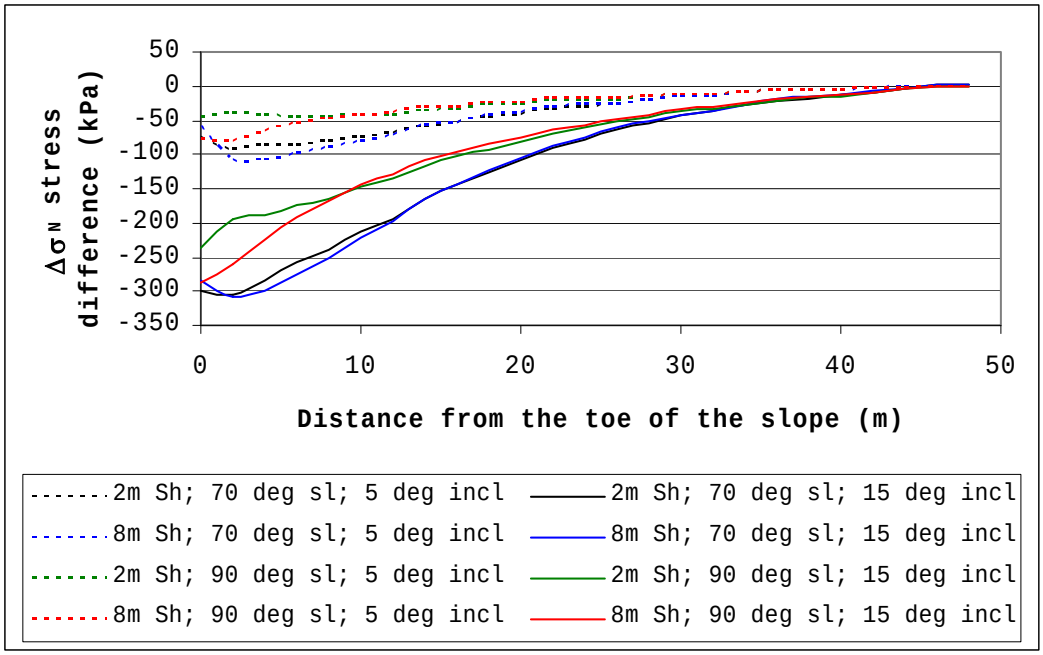

Figure 3.9

Induced stress changes normal to shale contact

The profiles with a vertical slope angle create a lower tensile difference than the profiles with a flatter slope angle in all investigated profiles. The figure shows that the stress difference normal to bedding is more or less proportional to the limb inclination.

These findings explain to some extent why a second collapse follows the initial slope failure that resulted in a reduction of the slope angle (see Example 1 in Chapter 1). From the stress difference results in Figure 3.9 we can conclude that the failures are related to stress relaxation normal to the strata. This aspect is investigated further in Chapter 4.

3.6 INVESTIGATION OF POTENTIAL PILLAR INSTABILITY AS A RESULT OF OPENCAST MINING

The current coal mine extracts all coal seams whether they were mined underground previously or not. As a result, the highwall slopes are cut above previously mined areas on the middle and bottom coal seams. The top seam was never mined by the underground coal mine. The highwall failures, presented in Chapter 1, appeared in areas where the underground mining activities didn't take place. For this reason, both highwall failures (discussed in Chapter 1) can not be associated with any influence on underground pillars. Hence, the following investigation of pillar instability as a result of opencast mining will discuss only the variations of the average induced pillar stress as a result of open cast mining.

The underground mining was exclusively bord and pillar, with pillar widths varying between 6.7 and 7.8m, and the bords averaging 6.7m in width for both seams. There was little data on average mining height in the old underground mine so an average of 3.5m, based on the stratigraphic column shown in Figure 1.3 and the previously used mining method "drill and blast", was

used. This assumes that either the middle or bottom coal seams were mined or if both were mined, they were mined to a height of approximately 1.5m each to leave a sufficiently thick middle parting. These mining parameters at about 45m depth give an approximate pillar safety factor ranging between 1.9 and 2.2, after the Collieries Research Laboratory (1972), which is based on the Salamon-Munro pillar strength formula. The extent of pillar failure prior to the open cast mining is not known, so it is likely that the average pillar safety factor was in the above calculated ranges.

The opencast pillar extraction sequence is shown in Figure 3.10, (deliberately omitting the buffer blasting step before cutting the slope, see below for description of buffer blasting) where the pillar numbering, and the profile line position at pillar mid-height, is shown. All the analyses of slopes established above mining on the middle coal seam assume the worst stability case in which the pillars remain intact after the slope has been cut. In reality, the mine practices buffer blasting, in which the pillars on the mined seam are shattered by drilling and blasting them from surface before the mine pit slope is cut. The reasons for carrying out buffer blasting are threefold:

1. buffer blasting will help to extinguish any pillars that might be burning through a process of spontaneous combustion;
2. if the pillars are still intact and not burning spontaneously, shattering them minimises the possibility that they could ignite spontaneously

when they are exposed to oxygen and water once the slope has been cut;

3. if pillar collapse below a slope were allowed after a slope had been cut, it could severely affect mining machinery both behind the slope crest and in the pit, and also affect spoil piles dumped behind the slope crest (see for example Figures 1.7 and 1.8).

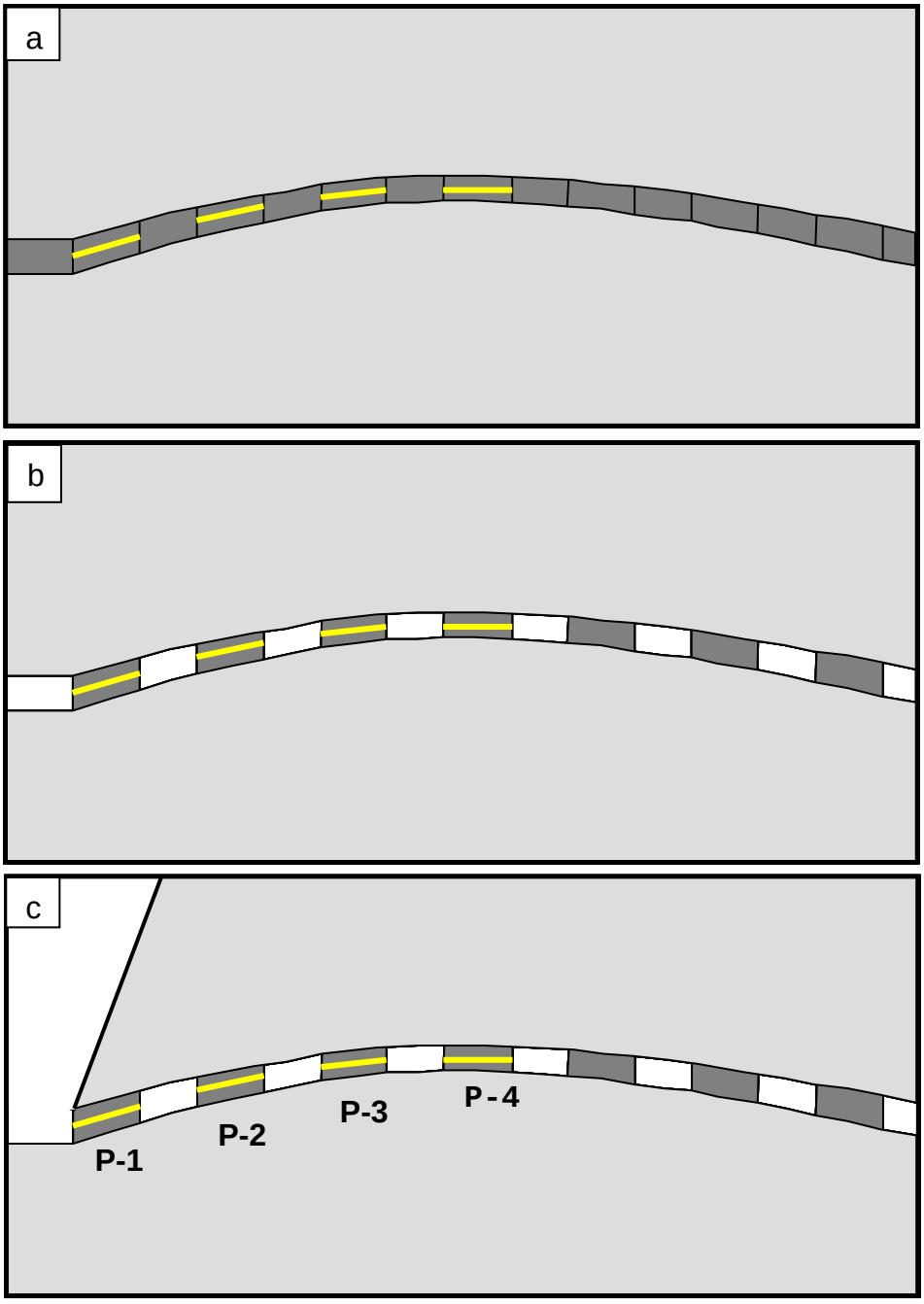

Figure 3.10

Profile lines (marked with yellow) for pillar stress analysis: a) virgin stress state; b) coal seam mined underground; and c) opencast exposure of coal pillars together with their numbers

Buffer blasting can only be carried out on the middle and bottom coal seams, because the top coal seam was never mined. If the buffer blasting is carried out perfectly, it would result in a layer of broken coal between 1.6 and 1.8m thick assuming a 1.6 swelling factor, 3.5m mining height, and areal extraction between 72 and 75% respectively. In all analyses, only a single mined seam was modelled.

In the pillar stress analyses, the average stress values along the pillar profile line are used, and the discussion that follows includes only results for the pillar geometry with a safety factor of 1.9, because the slope profile with pillar safety factor 2.2 shows similar results. These latter results appear in Appendix 3.

Table 3.4 Average inclination angles of the profile lines in the pillars

Pillar number	Profile line inclination angle (FOS=1.9 pillars)		Profile line inclination angle (FOS=2.2 pillars)	
	5^0	10^0*	5^0	10^0*
1	5	10	5	10
2	5	8	5	7
3	3	4	2	4
4	1	1	0	1

*The coal seams were not mined if the limb inclination was greater than 10^0.

Since the pillar profile lines are at different inclinations in each pillar, Table 3.4 shows the average inclination angles of the profile line at each pillar.

The effects of strata inclination on pillar stability are shown in Figures 3.11 and 3.12 using pillars with a safety factor of 1.9. The worst-case 90° slope angle has been used for this purpose (the slope above the middle coal seam in Figure 1.7 was actually 80°). As a two-dimensional program, FLAC assumes out-of-plane continuity of the profile. In order to account for the presence of bords around the pillars in both horizontal directions, the vertical pillar stress was doubled while out-of-plane stresses (horizontal and shear) were taken as calculated by FLAC.

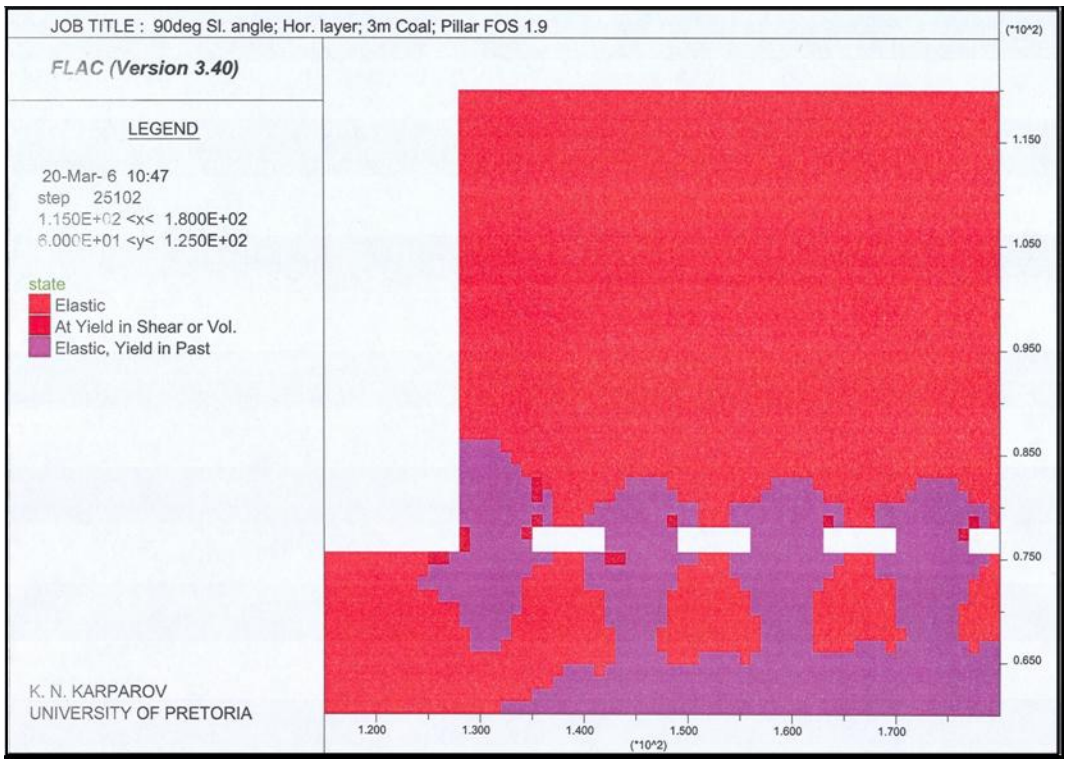

Figure 3.11

Pillar failure in flat strata below 90° slope

The model predicts some shear failure in the two pillars closest to the toe, with virtually no damage to pillars deeper in the slope. The slope overburden is in the elastic regime and damage to the enclosing strata due to the pillar failures is not present.

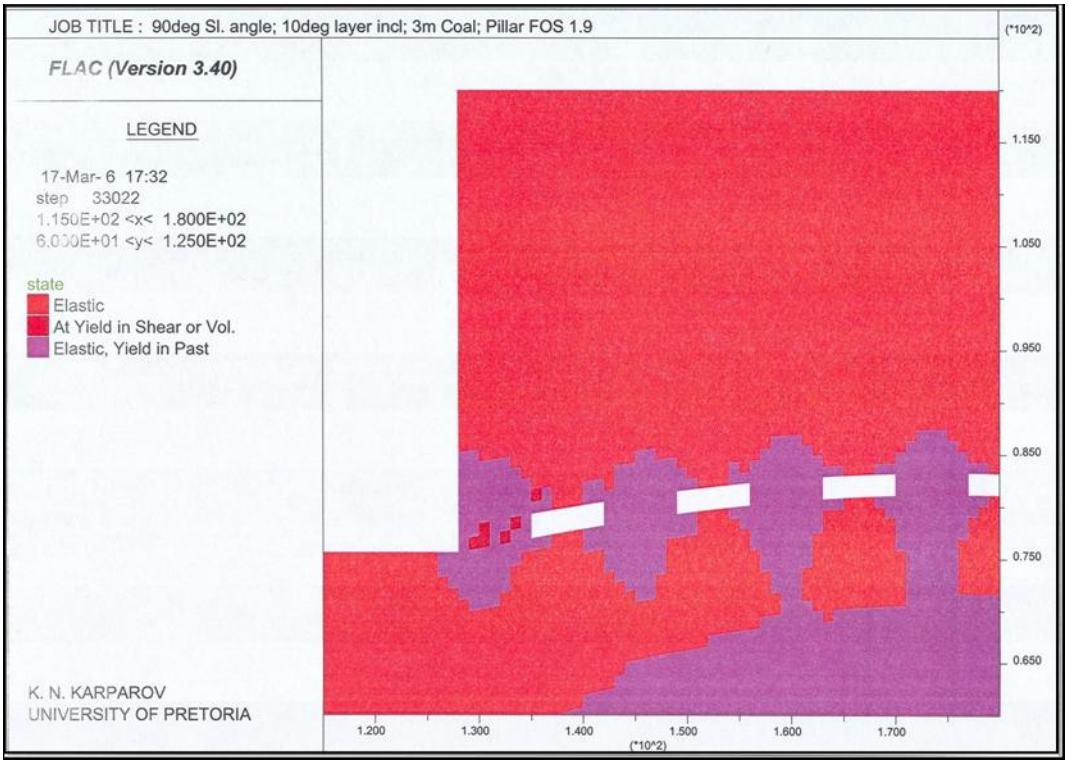

Figure 3.12
Pillar failure in inclined strata below 90° slope

Figure 3.12 shows the slope profile in inclined strata. In this case, only the pillar at the slope toe indicates some shear failure. Comparing this with the pillar failures predicted in flat strata, it appears that the pillars in the inclined strata may be more stable. This is probably because the coal layer thins on the limbs, giving the pillars a better width to height ratio if bord and pillar dimensions remain the same. Figures A2.17–A2.26 in Appendix 2 show pillar failure in all other possible scenarios.

For evaluation of underground pillar stability as a result of opencast extraction, the author uses induced stress components along the pillar mid-height between these two cases. The reasons for using underground

pillar scenario as a base for opencast extraction can be summarised as:

- Underground mining had taken place long time (about 30 years) before opencast mining. During this period, the stress state has achieved its balance and all possible deformations have taken place. One of these deformations is pillar scaling, which can be seen whenever the pillar is daylight in the toe of the slope.
- Both FLAC models (underground coal pillars with and without artificial slope) are with the same properties of strata and assumptions (regarding k-ratio). Hence, the stress state difference along the pillar mid-height is only result of the opencast extraction.
- Using induced stresses between both stages (FLAC models before and in time of opencast extraction) diminishes possible mistakes in the models regarding coal pillar properties (affected by scaling) or possible roof failures in bords.

Figure 3.13 presents a plot of the stress difference of the average vertical stress component ($\Delta\sigma_{YY}$) for the first four pillars in the slope profile at pillar mid-height. In the figure, the profile slope angle influences the average induced pillar vertical stress only in the first three pillars from the mining slope toe. The profile with a vertical slope angle has lower $\Delta\sigma_{YY}$ than the profile with a flatter slope angle. The slope profiles with steeper layer inclinations have lower $\Delta\sigma_{YY}$ values than the profiles with flatter strata inclination.

Since $\Delta\sigma_{YY}$ values always have a negative sign, the pillars undergo a decrease in vertical loading when the open cut approaches. Similar results hold for the pillar geometry with a safety factor of 2.2 (Figure A3.7, Appendix 3).

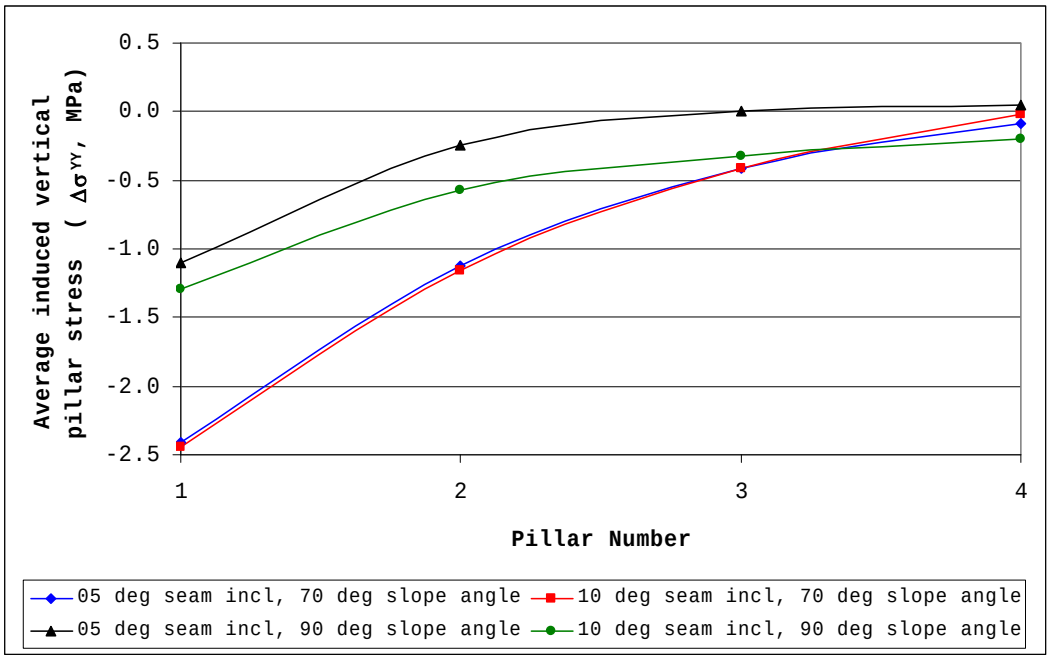

Figure 3.13
Induced vertical stress change in pillars at the base of the mined slope

Figure 3.14 shows a plot of the horizontal stress component difference ($\Delta\sigma_{XX}$) along the profile line. The graphs of the slope profiles with a pillar safety factor of 2.2 appear in Figure A3.8, Appendix 3. All values on $\Delta\sigma_{XX}$ are negative, which means a relaxation from the underground conditions. In Figures 3.13 and 3.14, it is seen that when the pillars approach the formation crest the average vertical and horizontal stress differences ($\Delta\sigma_{YY}$ and $\Delta\sigma_{XX}$) decrease in value in approximate proportion with the decreasing strata

inclination. The slope angle is insignificant for pillar numbers 2, 3 and 4 when considering induced horizontal stresses in the pillars.

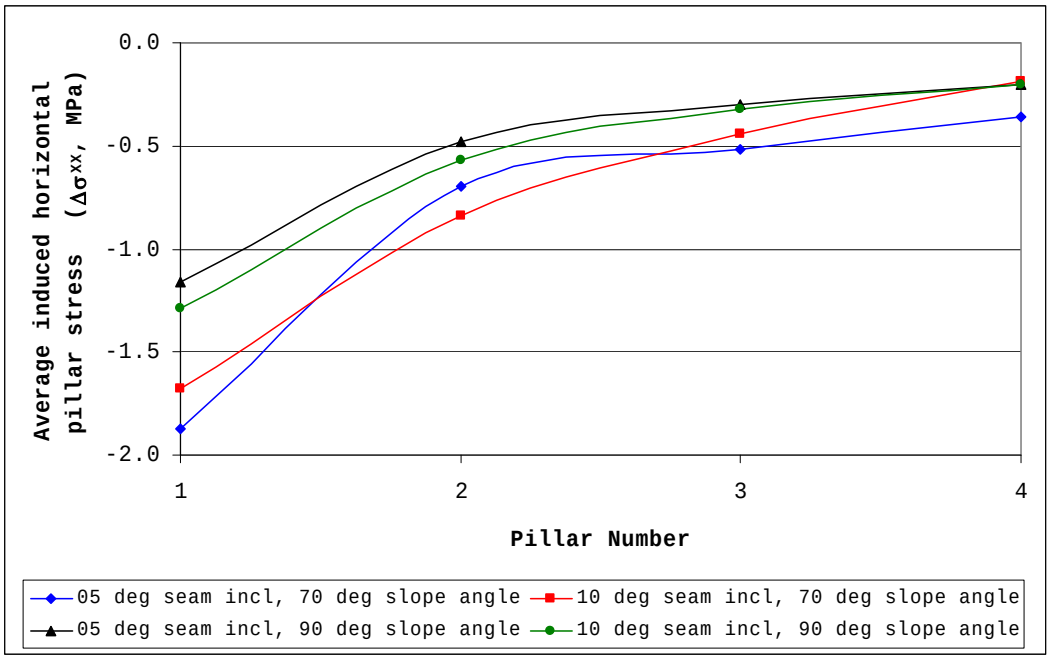

Figure 3.14
Induced horizontal stress change in pillars at the base of the mined slope

Along the formation limb shear stress changes ($\Delta\sigma_{XY}$), shown in Figure 3.15, do not differ significantly between the profiles with different layer inclinations. It is seen that opencast extraction of underground pillars increases the shear stress component in pillars. If we compare the profiles with different slope angles then the profile with the vertical slope maintains higher $\Delta\sigma_{XY}$ than the profile with flatter slope angle. Exception makes only pillar number one which has almost the same $\Delta\sigma_{XY}$ value in the profile with flatter slope angle profile compared to the profile with vertical slope angle at formation with flatter layer inclination. Comparing the shear stress

component difference from the graphs with different layer inclinations, the steeper formation has lower induced shear stress values than the formation with flatter limb inclination. Shear stress changes for the profiles with pillar safety factor 2.2 appear in Figure A3.9, Appendix 3.

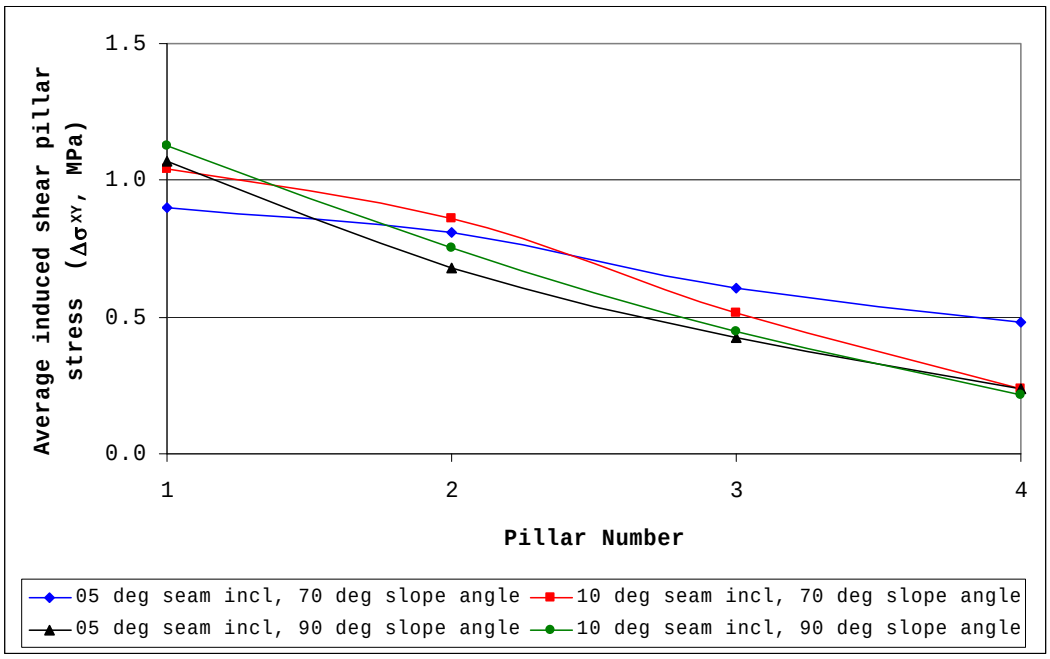

Figure 3.15
Induced shear stress change in pillars at the base of the mined slope

Shen and Duncan Fama (1999) investigated the highwall mining experience in Australia, where mines using the Continuous Highwall Mining System create rectangular entries, usually 3.5m wide, with a distance of 2.5m between entries. Every 3 to 5 entries, barrier pillars 5-8m wide are left. In this situation, mainly roof failures were observed, while subsided zones and highwall failures also occurred, but more rarely (Shen and Duncan Fama, 1999).

Generally, the Australian pillar safety factors are lower than for this study, so we can draw the conclusion that the highwall failures as a result of opencast pillar extraction in the South African coal mine are unlikely, and become extremely improbable because of the buffer blasting of pillars prior to slope excavation. Although the pillar model appears stable as modelled, it will be more stable if the buffer blasted pillars were modelled as a 1.6-1.8m cohesionless coal seam with zero tensile strength. The bulk and shear moduli would be about half the values given in Table 3.1, while the density would be reduced to 1000kg/m^3 because of the bulking factor. A lithostatic stress state would also have to be modelled within the coal seam, which would be impossible in FLAC if other parts of the profile are not in a lithostatic stress state. Finally, buffer blasting has been confirmed by experience at the mine as being effective in maintaining slope stability in slopes above pillars, so it is concluded that the pillars have played no role in the slope collapses observed on the shale-top coal seam contact, since all major failures described in Chapter 1 were on the contact between the shale and the unmined middle coal seam.

3.7 CONCLUSIONS

The following conclusions can be drawn from the simple models tested in this chapter:

- Stress relaxation normal to bedding occurs when the mine slope has been cut.

- Normal pillar stresses are reduced by the slope, but this relaxation is insufficient to cause pillar instability.
- Observations at the mine showed that no mining took place in coal seams inclined at 10° or more, and that the top coal seam was never mined by the underground mine.
- The models help to confirm that pillars below slopes will probably not have an effect on slope stability.
- The models used are unable to completely explain why major slope failures occurred in slopes located above unmined ground, but their results can be used as input for the development of a proposed block thrust mechanism described in Chapters 5 and 6.

Since the models on their own are unable to confirm slope failure above unmined undulating coal seams, investigation into the mechanisms through which failure can eventually result along the shale-middle coal seam contact are indicated, and are discussed in Chapter 4.